ECLÉTICA QUÍMICA

Eclet. Quim. 51 | e-1660, 2026

Original Articles in Chemistry and Related Areas

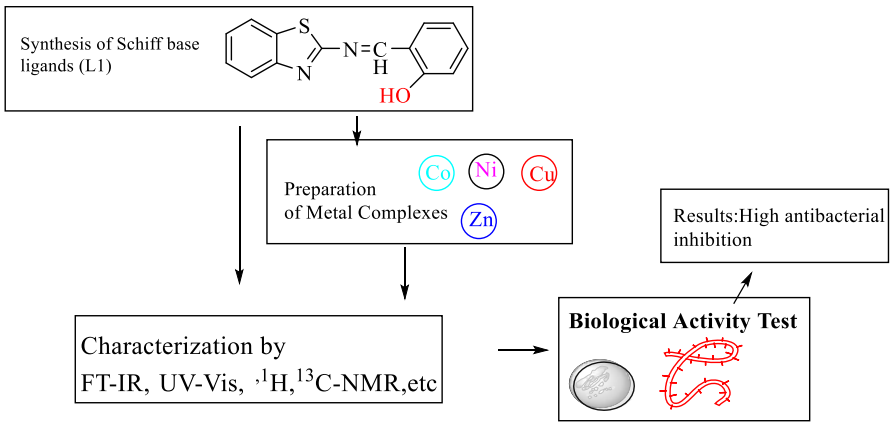
https://doi.org/10.26850/1678-4618.eq.v51.2026.e1660

Preparation and characterization of some transition metal complexes Co(II), Ni(II), Cu(II), and Zn(II) with a Schiff base ligand and study of their biological activity

Sondos Ibrahim **Atallah**[1], Fadia Jalal **Ahmed**[1+]

Abstract

A new Schiff base, 2-((benzo[d]thiazol-2-ylimino)methyl)phenol (L1), was synthesized via condensation of 2-hydroxybenzaldehyde with 2-aminobenzothiazole. Complexes of L1 with Co(II), Ni(II), Cu(II), and Zn(II) were prepared and characterized using various techniques, including elemental analysis (CHNS), infrared (FTIR), UV-visible (UV-Vis) and nuclear magnetic resonance (^{1}H, ^{13}C NMR) spectroscopies, thermogravimetric analysis (TGA), magnetic susceptibility, atomic absorption (AAS), molar conductivity, and melting point. The results suggested an octahedral geometry for the complexes and a 1:2 electrolytic nature. The biological activity of the ligand and its complexes was tested, and significant antibacterial activity against selected bacterial strains was observed.



Article History

Received April 19, 2025
Accepted August 08, 2025
Published November 11, 2026

Keywords

1. Schiff bases;
2. transition metal complexes;
3. coordination chemistry;
4. spectroscopic analysis;
5. antibacterial activity.

Section Editors

Assis Vicente **Benedetti**

Highlights

- Complexes show octahedral geometry based on magnetic and spectral data.
- Complexes exhibit strong activity against Gram-positive and Gram-negative bacteria.
- Thermal analysis indicates high stability and anhydrous decomposition behavior.

[1]University of Mosul, College of Education for Pure Science, Mosul, Iraq. **+Corresponding author:** Fadia Jalal Ahmed, **Phone:** +9647719825418, **Email address:** fadiaa374@uomosul.edu.iq

creative commons

1. Introduction

Schiff bases are organic compounds containing an azomethine group (C=N). They are named after the Italian scientist Hugo Schiff, who produced them in 1864 by a condensation reaction between aldehydes or ketones and primary amines ((Almáši *et al.*, 2021; Hamil *et al.*, 2024);. Schiff bases are characterized by different names, depending on the nature of each of R1, R2, and R3. Schiff bases are imines, azomethines, benzanilides, benzylidene anilines, or naphthylidene anilines. They are also called ketamines when they are derived from ketones. Aldimines are derived from aldehydes (Paul and Hossen, 2020). Schiff bases can be classified according to the donor sites into monodentate, bidentate, tridentate, and multidentate (Alkam, 2017; Rana *et al.*, 2009; Srivastava *et al.*, 2014). Schiff bases are of great importance in coordination chemistry because of their ability to form stable and diverse complexes with different shapes and properties, especially with varying transition elements. It was found that most of the transition metal ions with the ligands of Schiff bases form stable complexes, which can coordinate with metals through both nitrogen and oxygen atoms. Because of the biological importance of Schiff bases, they play a significant role in the Schiff base complexes with Pd(II) (Khalil *et al.*, 2021; Raj *et al.*, 2023). Schiff bases and their complexes also play a significant role in various chemistry, biology, and medicine fields. Therefore, recent studies have been conducted on the coordination chemistry and biological effects of mixed ligand complexes of Pd(II), Zn(II), and Cd(II) (Dalia *et al.*, 2018; Radhi *et al.*, 2023). There are multiple methods and modern preparation techniques, some of which have been documented and are as follows: the traditional heating method, the use of ultrasound, the use of basic medium, and the use of microwaves in preparing Schiff bases (Mukhtar *et al.*, 2021).

Also, researchers (Oladipo and Luckay, 2024) were able to prepare two new lipophilic bases: (E)-1-(((2,6-chlorophenyl)imino)methyl)naphthalen-2-ol and (E)-1-(((4-bromo-2,6-dichlorophenyl)imino)methyl)naphthalen-2-ol. They were prepared by mixing equal proportions of the reactants and escalating the mixture for 6 h. Then, copper complexes were prepared by reacting to the two bases with copper nitrate trihydrate. The ligands and their metal complexes were also characterized using infrared (IR), ultraviolet-visible (UV-VIS), and ^{1}H and ^{13}C nuclear magnetic resonance (^{1}H,^{13}C-NMR) spectroscopy, in addition to studying the mass spectrum and elemental analysis. Electron magnetic resonance (EPR) was used to confirm the magnetic nature of complexes 1 and 2 and to study the crystal structure using X-rays diffractometry (XRD) for both complexes 1 and 2. Studies have confirmed the formation of mononuclear complexes. The metal ion, Cu(II), is linked with two Schiff bases via the nitrogen atom of the azomethine group and the oxygen atom of the alcohol group. The prepared complexes took the form of a planar, slightly distorted square. The effectiveness of the complexes against certain types of bacteria was tested, as well as their effectiveness as antidiabetics (Oladipo and Luckay, 2024).

In this study, a new Schiff base ligand 2-((benzo[d]thiazol-2-ylimino)methyl)phenol was prepared by condensation reaction between 2-hydroxybenzaldehyde, and 2-aminobenzothiazole, and then four new transition metal complexes were prepared, including cobalt(II), nickel(II), copper(II) and zinc(II) using the prepared Schiff base ligand (Khalil and Abdullah, 2024). The prepared compounds were characterized by different methods such as elemental analysis (CHNS), infrared (FTIR) and UV-Visible (UV-Vis) spectroscopy, ^{1}H-, ^{13}C-NMR, thermogravimetric analysis (TGA), magnetic susceptibility, atomic absorption, molar conductivity, and melting point. The measurement results showed that all the complexes were in octahedral shape. The activity of the prepared complexes against a variety of gram-positive and gram-negative bacteria was also studied, and the results showed that the complexes have good biological activity (Abed *et al.*, 2020).

2. Experimental

2.1. Reagents and solutions

Fluka, Aldrich, and BDH companies prepared the materials used: 2-hydroxybenzaldehyde, 2-aminobenzathiazole, 4-hydroxybenzaldehyde, the solvents absolute ethanol, diethyl ether, petroleum ether, and the metallic salts $CoCl_2.6H_2O$, $NiCl_2.6H_2O$, $CuCl_2$, and $ZnCl_2$.

2.2. Instrumentation

The ligand and its complexes were detected by various measurements: Molar conductivity was measured using a Conductivity Meter-Model (Eutech PC700) device, and a Magnetic Susceptibility Balance device to measure effective magnetic moment. UV-Vis spectrophotometer (PG INSTRUMENTS) was used to measure electronic spectra. Both standards are available at the University of Mosul, College of Education for Pure Sciences. The infrared spectra of the prepared complexes and ligand were determined using a Shimadzu type device in the range 200 - 4000 cm^{-1} in terms of wavenumber and by using CsI disks at Tikrit University, College of Education for Pure Sciences. Mass-spectrum measurement was performed using a USA-Agilent device at the University of Tehran in Iran. Thermogravimetric analysis was conducted using a METTLER TOLEDO device at the University of Mosul, College of Basic Education. The thin-layer chromatographic analysis was performed using a TLC slide in a UVG-11 Compact UV Lamp, Varian Agilent USA, 400 MHz device with hexane and ethyl acetate solvents at the College of Education for Pure Sciences, University of Mosul. ^{1}H-NMR and ^{13}C-NMR measurements of the prepared ligand were conducted at the University of Basra, College of Education for Pure Sciences, using a Varian Agilent USA 400 MHz device. The samples were dissolved in DMSO-d^6, using TMS as a standard reference at room temperature (298 K). Accurate element analysis was conducted to estimate the proportions of carbon, hydrogen, nitrogen, and sulfur elements in the prepared compounds and complexes using an elemental analysis instrument at the University of Tehran in Iran. The amounts of cobalt, nickel, copper, and zinc in the prepared complexes were determined using an atomic absorption spectrometer (Analytik Jena Novaa350) at the University of Mosul, College of Agriculture. Finally, the melting point of raw materials, prepared ligand, and their complexes were measured using an Apparatus-Stuart-SMP melting point device at the University of Mosul, College of Education, Pure Sciences.

2.3. Preparation of microparticles

2.3.1. Synthesis of ligand (L1)

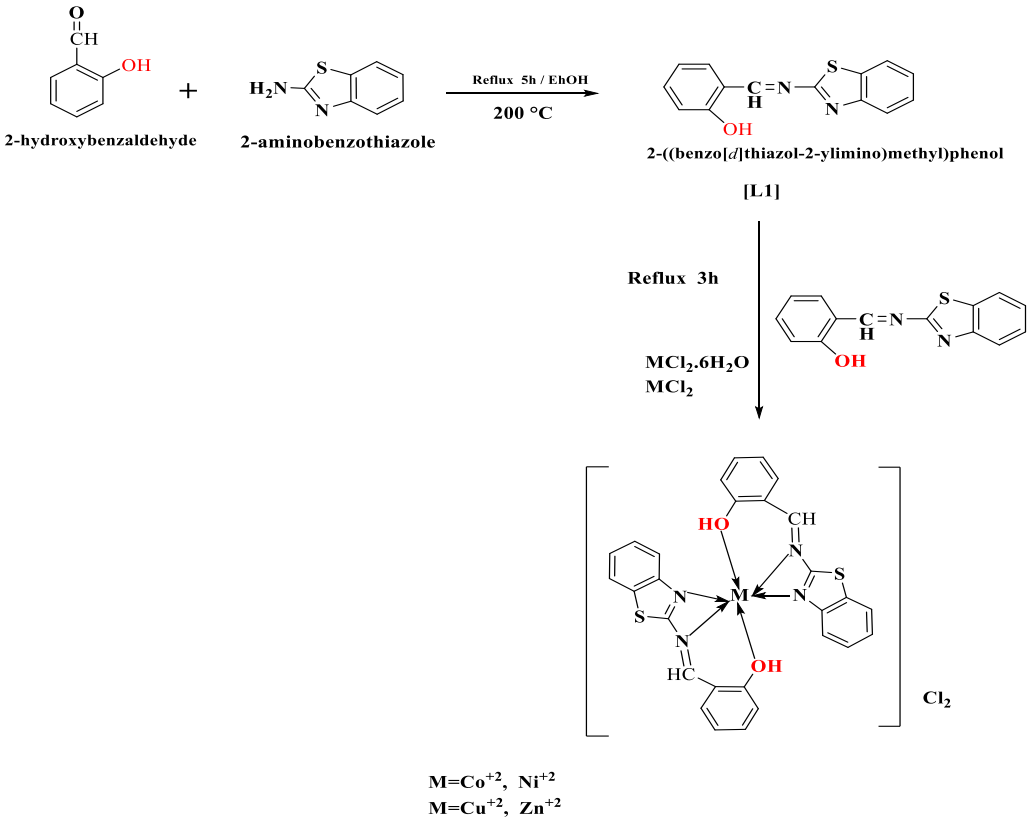
The ligand was prepared by adding (0.02 mol, 2.80 g) of 2-hydroxybenzaldehyde dissolved in (20 mL) of absolute ethanol to (0.02 mol, 3.00 g) of 2-aminobenzothiazole, also dissolved in (20 mL) of absolute ethanol. The reaction mixture was refluxed for 5 h (**Scheme 1**). A yellow precipitate was formed. It was

recrystallized and washed first with distilled water and then with diethyl ether. Its melting point was 120 °C (Ahmed *et al.*, 2022).

2.3.2. Preparation of ligand complexes with the formula $[M(L1)_2]Cl_2$

The cobalt complex was prepared in a ratio of (1:2) by reacting (0.001 mol, 0.237 g) of the metal salt $CoCl_2.6H_2O$ dissolved in (10 mL) distilled water with (0.002 mol, 0.508 g) of ligand (L1) after dissolving it in 25 mL absolute ethanol and was refluxed for 3 h. Later, it forms a bright blue precipitate with a melting point of 100 °C.

In the same way, the nickel complex was prepared using 0.237 g of $NiCl_2.6H_2O$ and 0.136 g of $CuCl_2$, $ZnCl_2$, using the same weights for the ligand. **Scheme 1** shows the sequency for the synthesis of ligand and metal complexes.



Scheme 1. Ligand and its metallic complexes preparation.
Source: Elaborated by the authors.

3. Results and discussion

3.1. Molar conductivity

The complexes were dissolved in (DMF) at a concentration of (10^{-3} mol L^{-1}), where molar electrical conductivity measurements showed agreement with the proposed structural formulas of the prepared compounds, as they were conductive at a ratio of (1:2), as shown in **Table 1**. To confirm the electrolytic nature of the complexes, molar conductivity measurements were also carried out in dimethyl sulfoxide (DMSO) in addition to DMF. The observed conductivity values in DMSO were comparable to those in DMF, indicating that the complexes exhibit similar 1:2 electrolytic behavior in both solvents and likely dissociate into $[M(L1)_2]^{2+}$ and two chloride ions in solution. This is consistent with published research (Knittl *et al.*, 2018; Sultan *et al.*, 2024).

Table 1. The formula, the complex's physical characteristics, molar conductivity, and elemental analysis.

NO	Formula of complexes	Molecular Weight (g mol^{-1})	Color	M.P (^{0}C)	Molar conductivity (cm^2 Ω^{-1} mol^{-2})		Yield	Elemental analysis theoretical (Practical)				
					DMF	DMSO		C%	H%	N%	S%	M%
L1	$C_{14}H_{10}N_2SO$	254.3	Dark yellow	160	---	---	86%	66.12 (66.05)	3.96 (3.71)	11.02 (11.00)	12.61 (12.43)	---
1	$[Co(L1)_2]Cl_2$	638.5	Shiny Blue	001	143	85	89%	52.67 (52.61)	3.13 (3.11)	8.77 (8.71)	10.03 (10.00)	9.23 (9.19)
2	$[Ni(L1)_2]Cl_2$	683.2	Light Earth Green	101	150	65	87%	52.69 (52.56)	3.13 (3.07)	8.78 (8.76)	10.03 10.00)(	9.19 (9.13)
3	$[Cu(L1)_2]Cl_2$	643.1	Light Olive	98	165	73	93%	52.29 (52.25)	3.11 (3.07)	8.71 (8.68)	9.96 (9.92)	9.88 (9.83)
4	$[Zn(L1)_2]Cl_2$	644.9	Light Yellow	94	155	70	92%	52.14 (52.11)	3.10 (3.08)	8.69 (8.67)	9.93 (9.90)	10.13 (10.09)

Source: Elaborated by the authors.

3.2. Magnetic susceptibility measurements

The magnetic susceptibility of the prepared complexes was measured, and the results are consistent with an octahedral geometry for all metal centers. The Co(II) complex exhibited a magnetic moment of 4.9 BM (1 BM = 9.274×10^{-24} J T^{-1}), which is higher than the spin-only 3.87 BM value due to orbital contribution and spin–orbit coupling effects typical of high-spin octahedral Co(II) complexes (Zahradnikova *et al.*, 2024). The Ni(II) complex showed a magnetic moment of 2.8 BM, consistent with two unpaired electrons in an octahedral field. The Cu(II) complex exhibited a moment of 1.8 BM, in agreement with a single unpaired electron in a distorted octahedral geometry, possibly affected by Jahn-Teller distortion. The Zn(II) complex was diamagnetic, as expected for a d^{10} closed-shell configuration. These magnetic data, together with spectral features (UV-Vis, IR), support the proposed octahedral coordination geometry. This is consistent with published research (Abed *et al.*, 2020; Abousaty *et al.*, 2024; Adnan *et al.*, 2024).

3.3. Atomic absorption

The proportions of Co, Ni, Cu, and Zn elements in the resulting complexes were estimated based on Table 1. Compared with the theoretically calculated values, the resulting complexes agreed with the proposed formulas (Ismail and Lateef, 2022).

3.4. Elemental analysis (CHNS)

Elemental analysis is performed on the isolated complexes to confirm their composition, and the results obtained from this analysis are shown in Table 1. The results in Table 1 show a good agreement between the calculated and experimental ratios of the elements C, H, N, and S for the proposed composition. This agreement enhances the validity of the composition of the synthesized complexes (Abed *et al.*, 2021; Ismail and Lateef, 2022).

3.5. Electronic spectra studies

In this study, the electronic spectra of the ligand and the prepared complexes were measured using dimethylformamide as solvent at a concentration of (10^{-3} mol L^{-1}) and using two cells with a diameter of (1 cm) (Figs. 1–5). The prepared complexes gave bands for the (d–d) transitions as well as the charge transfer bands, and the high-intensity absorption appearing in the region of 35849 to 42216 cm^{-1} are due to the intra-ligand transitions ($\pi \rightarrow \pi*$, $n \rightarrow \pi*$), the complex Co(II) exhibit a three absorption bands in the 11185-21881cm^{-1} range, which were attributed to $^4T_1g(F) \rightarrow {}^4T_2g(F)$, $^4T_1g(F) \rightarrow {}^4A_2g(F)$, and $^4T_1g(F) \rightarrow {}^4T_1g(P)$ octahedral transitions sequentially (Table 2). Although these transitions are Laporte-forbidden due to the centrosymmetric octahedral environment, they appear with moderate intensity due to vibronic coupling and slight distortions in the geometry. The UV-Vis spectrum of Ni(II) complex exhibits three absorption bands in the 10659-22431cm^{-1} range, which were attributed to $^3A_2g(F) \rightarrow {}^3T_2g(F)$, $^3A_2g(F) \rightarrow {}^3T_1g(F)$, and $^3A_2g(F) \rightarrow {}^3T_1g(P)$ octahedral transitions sequentially.

The hexa-coordinated Cu(II) complex showed a single absorption band in the 12820–13989 cm^{-1} range due to the transition $^2Eg \rightarrow {}^2T_2g$, which is characteristic of the $^2Eg \rightarrow {}^2T_2g$ transition in an octahedral geometry distorted by Jahn–Teller effect. This distortion leads to axial elongation and splitting of degenerate orbitals, resulting in an asymmetric and broadened absorption band. The broadness of the bands in all complexes is further attributed to: Overlapping of electronic transitions, and spin–orbit coupling, especially in the Co(II) complex. These spectral features, combined with magnetic moment values, support the octahedral geometry assigned to the complexes. It conforms to an octahedral geometric shape. As for the Zn(II) complex, the outer shell is filled with electrons, and then, no electronic transition bands (d-d) appear. Still, it gives bands related to the ligand electronic transitions, whose positions have changed from those in the ligand spectrum, indicating the formation of a complex (Adnan *et al.*, 2024; Ommenya *et al.*, 2020).

Table 2. Data on the electronic spectra and effective magnetic moment of the ligand and prepared complexes.

NO	Formula of complexes	μ_{eff} B.M	UV-Vis. Bands (cm^{-1})	Charge transfer (cm^{-1})	Proposed structure
L1	$C_{14}H_{10}N_2SO$	----	----	35849; 42216	----
1	$[Co(L1)_2]Cl_2$	4.9	21881;11185; 15625	35714	Octahedral
2	$[Ni(L1)_2]Cl_2$	2.8	22431; 20897;10659	32576	Octahedral
3	$[Cu(L1)_2]Cl_2$	1.8	11160	34722	Octahedral
4	$[Zn(L1)_2]Cl_2$	Dia	----	34246	Octahedral

Source: Elaborated by the authors.

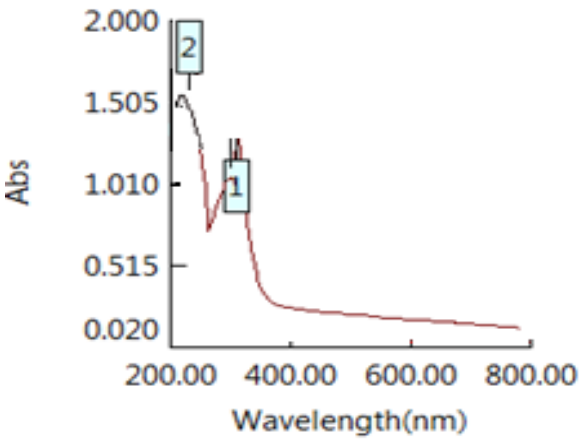


Figure 1. UV-Vis spectrum of the ligand.
Source: Elaborated by the authors.

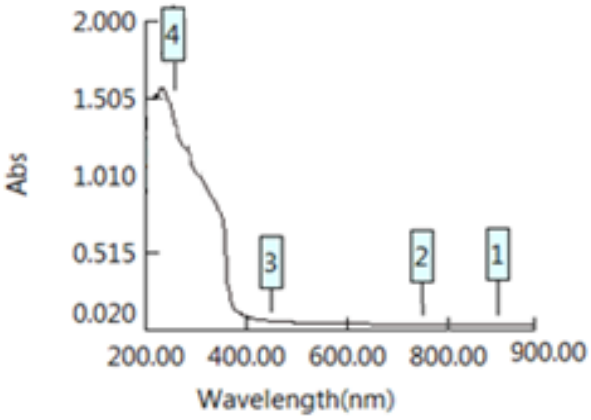


Figure 2. UV spectrum of the complex $[Co(L1)_2]Cl_2$.
Source: Elaborated by the authors.

https://doi.org/10.26850/1678-4618.eq.v51.2026.e1660

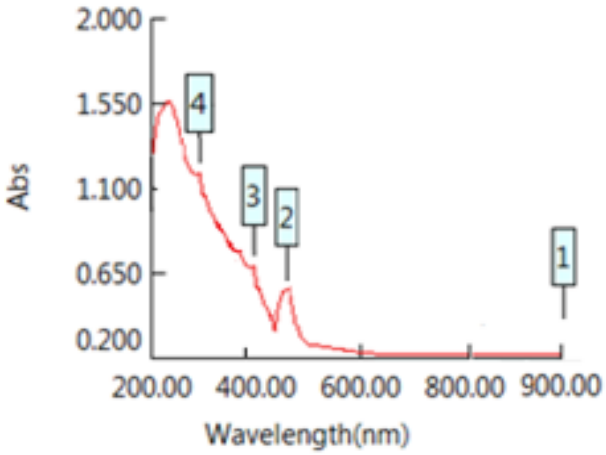


Figure 3. UV spectrum of the complex $[Ni(L1)_2]Cl_2$.
Source: Elaborated by the authors.

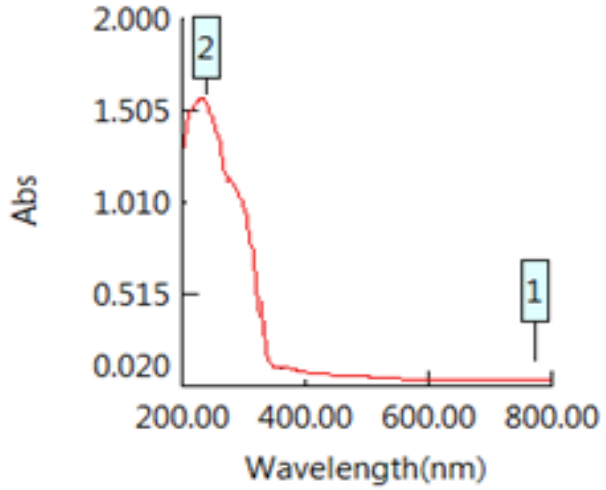


Figure 4. UV spectrum of the complex $[Cu(L1)_2]Cl_2$.
Source: Elaborated by the authors.

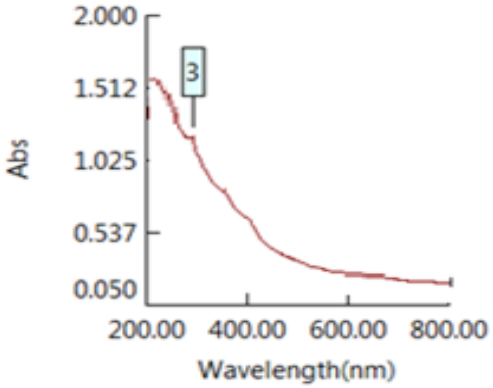


Figure 5. UV spectrum of the complex $[Zn(L1)_2]Cl_2$.
Source: Elaborated by the authors.

3.6. IR spectra studies

FTIR spectra (**Figs. 6–10**) indicate that the coordination in the complexes is mediated by the two nitrogen atoms in the (C=N) groups, without the participation of sulfur from the (C-S) group. A shift in the (C=N) vibration bands to lower values compared to the free ligand is observed, indicating that both the extra- and intra-ring imine bonds participate in the coordination. In contrast, no significant spectral shift is observed in the C-S band, indicating that the sulfur atom is not involved in coordination with the metal. We also note that the values of the (OH) group have shifted to lower values. Based on these spectroscopic results, we conclude that the coordination is mediated by the two nitrogen atoms and the oxygen atom, i.e., the ligand is tridentate coordinated. We also note the appearance of new bands associated with (M-N, M-O, M-Cl) at ranges (321-393 cm^{-1}, 583-574 cm^{-1}, 251-279 cm^{-1}), which confirms the occurrence of coordination (**Table 3**). As for the thiol/thiol equilibrium, we explain that the sulfur in the ligand is part of a stable aromatic benzothiazole ring and does not exist in the form of C=S (thione) or –SH (thiol), so this type of equilibrium is not possible in this system. This was supported by the absence of any S–H stretching band in the infrared spectrum (Ahmed *et al.*, 2022; Tahmasbi *et al.*, 2023).

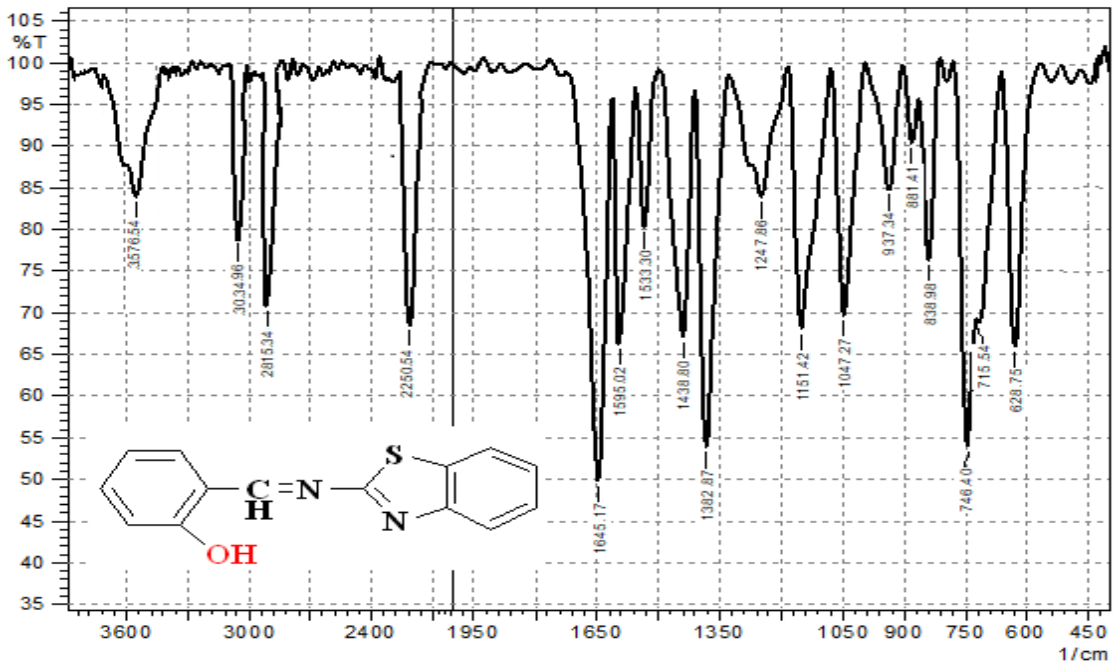


Figure 6. Infrared spectrum of the ligand ($C_{14}H_{10}N_2SO$).
Source: Elaborated by the authors.

https://doi.org/10.26850/1678-4618.eq.v51.2026.e1660

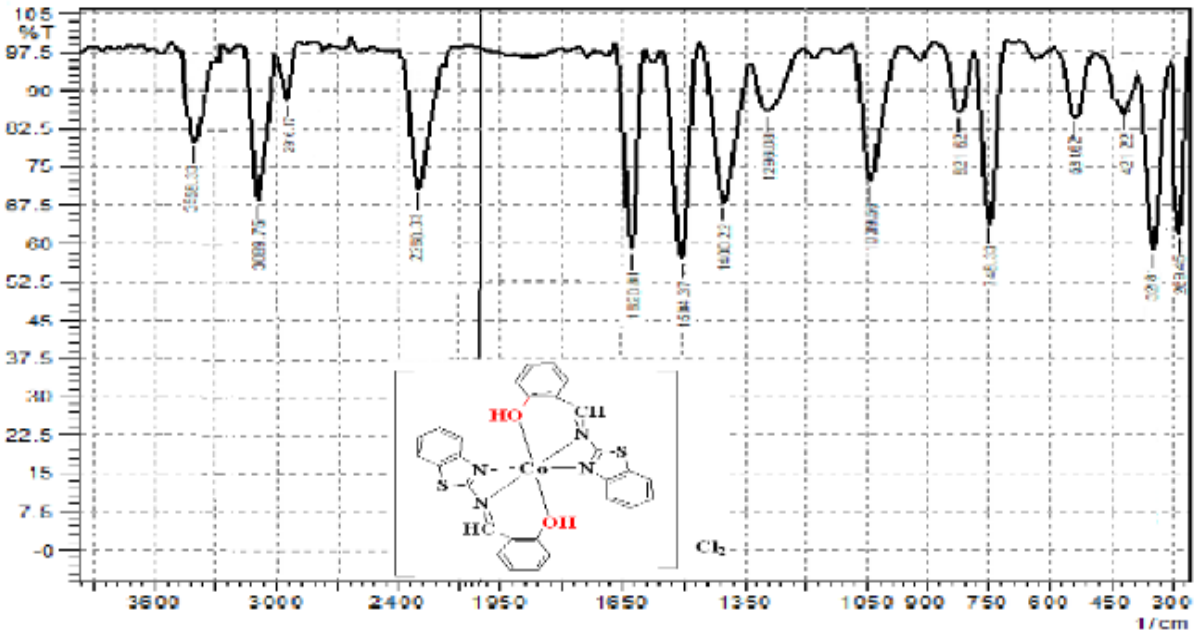


Figure 7. Infrared spectrum of the complex $[Co(L1)_2]Cl_2$.
Source: Elaborated by the authors.

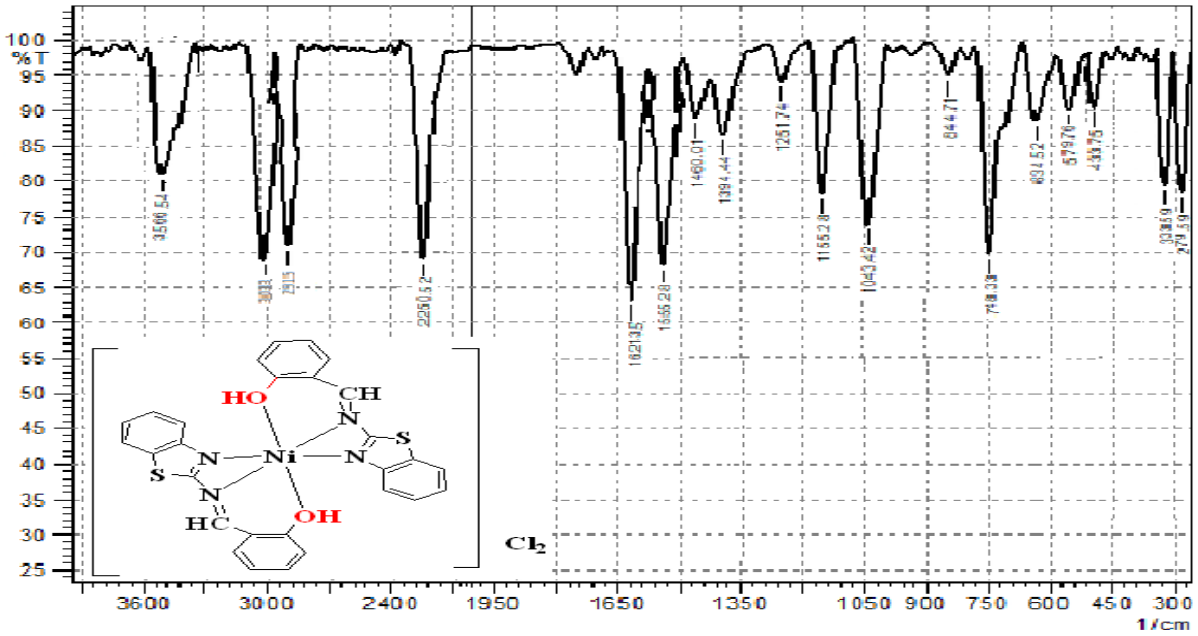


Figure 8. Infrared spectrum of the complex $[Ni(L1)_2]Cl_2$.
Source: Elaborated by the authors.

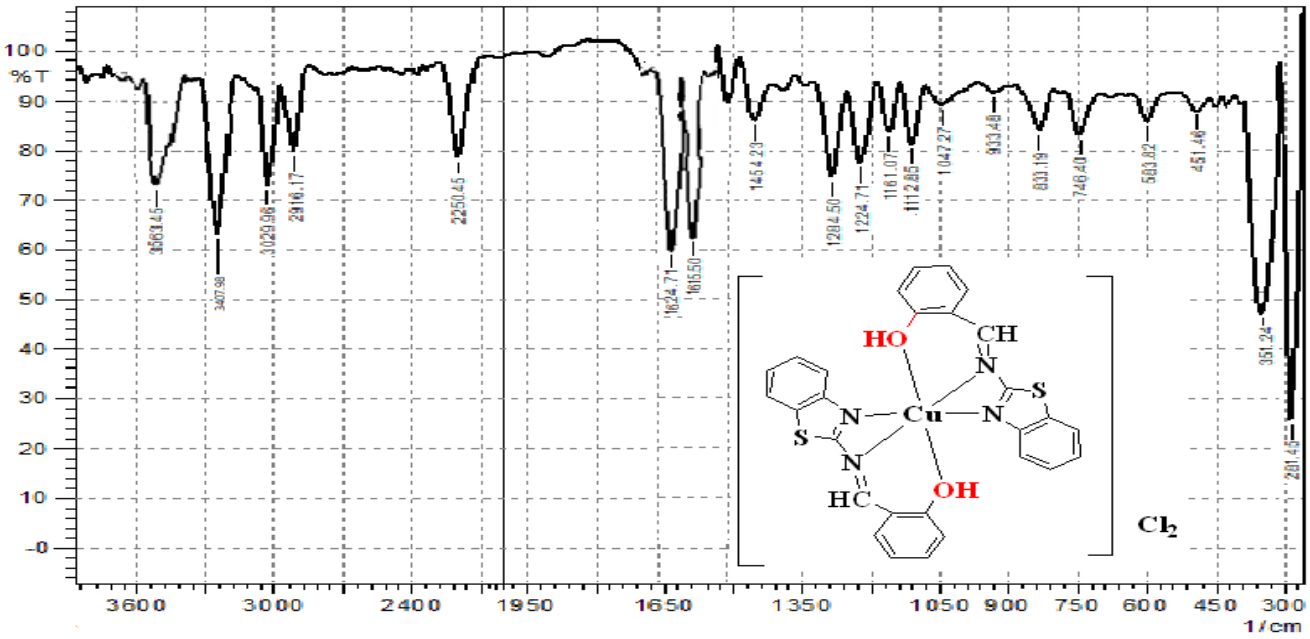


Figure 9. Infrared spectrum of the complex $[Cu(L1)_2]Cl_2$.
Source: Elaborated by the authors.

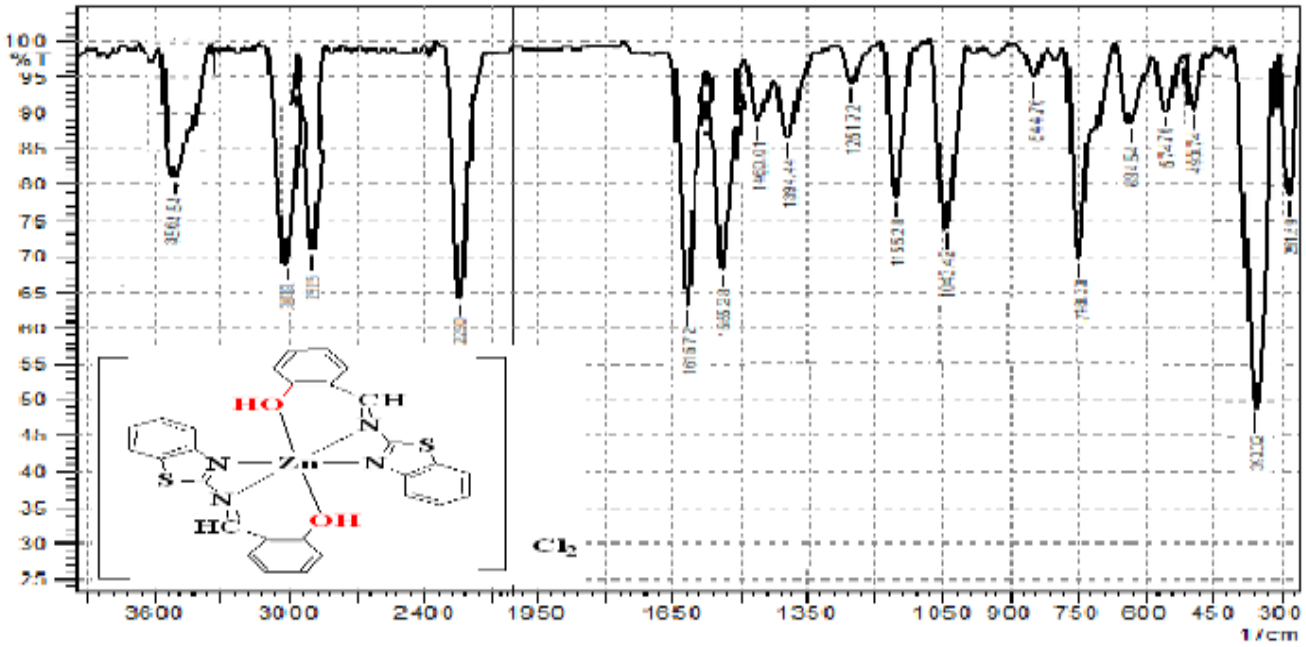


Figure 10. Infrared spectrum of the complex $[Zn(L1)_2]Cl_2$.
Source: Elaborated by the authors.

Table 3. IR bands (cm^{-1}) data of the ligand and prepared complexes.

N0	Formula of complexes	ν(-OH)	ν(N=C-S)	ν(C-S)	ν(C=N)	ν(M-O)	ν(M-N)	ν(M-Cl)
L1	$C_{14}H_{10}N_2SO$	3576	2254	1151	1645	---	---	---
1	$[Co(L1)_2]Cl_2$	3558	2220	1154	1620	581	321	269
2	$[Ni(L1)_2]Cl_2$	3566	2227	1155	1621	579	333	279
3	$[Cu(L1)_2]Cl_2$	3563	2234	1153	1615	583	351	281
4	$[Zn(L1)_2]Cl_2$	3564	2237	1155	1612	574	393	251

Source: Elaborated by the authors.

3.7. ^{13}C, ^{1}H-NMR

The ligand ^{1}H-NMR spectra are recorded using deuterated dimethyl sulfoxide as an internal reference. The ^{1}H-NMR spectrum (**Fig. 11**) of the ligand (L1) showed ^{1}H-NMR ($CDCl_3$, 400 MHz) δH (ppm) **8.04-6.97** (8H,m, Ar-H)) with an integration value of 5.77, **8.89** (1H,S, H-C=N) with an integration value of 0.68 11.04 (1H, S, OH) with an integration value of 0.67. **8.89**(1H,S, H-C=N) 11.04(1H, S, OH) (Butera *et al.*, 2023; Uttu *et al.*, 2022).

As for the ^{13}C-NMR spectrum of the ligand L1 (**Fig. 12**), it only showed a peak belonging to the carbon atom of the azomethine group, and it was at a frequency of (153.19 ppm), as

well as the carbon atom of the thiazole ring, which gave a peak at (166.95 ppm), the carbon atom connected to the thiazole ring from the nitrogen atom (148.99 ppm), peak at the (161.59 ppm) for the hydroxyl group belongs to the carbon atom, and multiple peaks in the region between (118.17-133.02 ppm) for the carbon atoms of the aromatic rings (Afifi *et al.*, 2025; Soliman *et al.*, 2022).

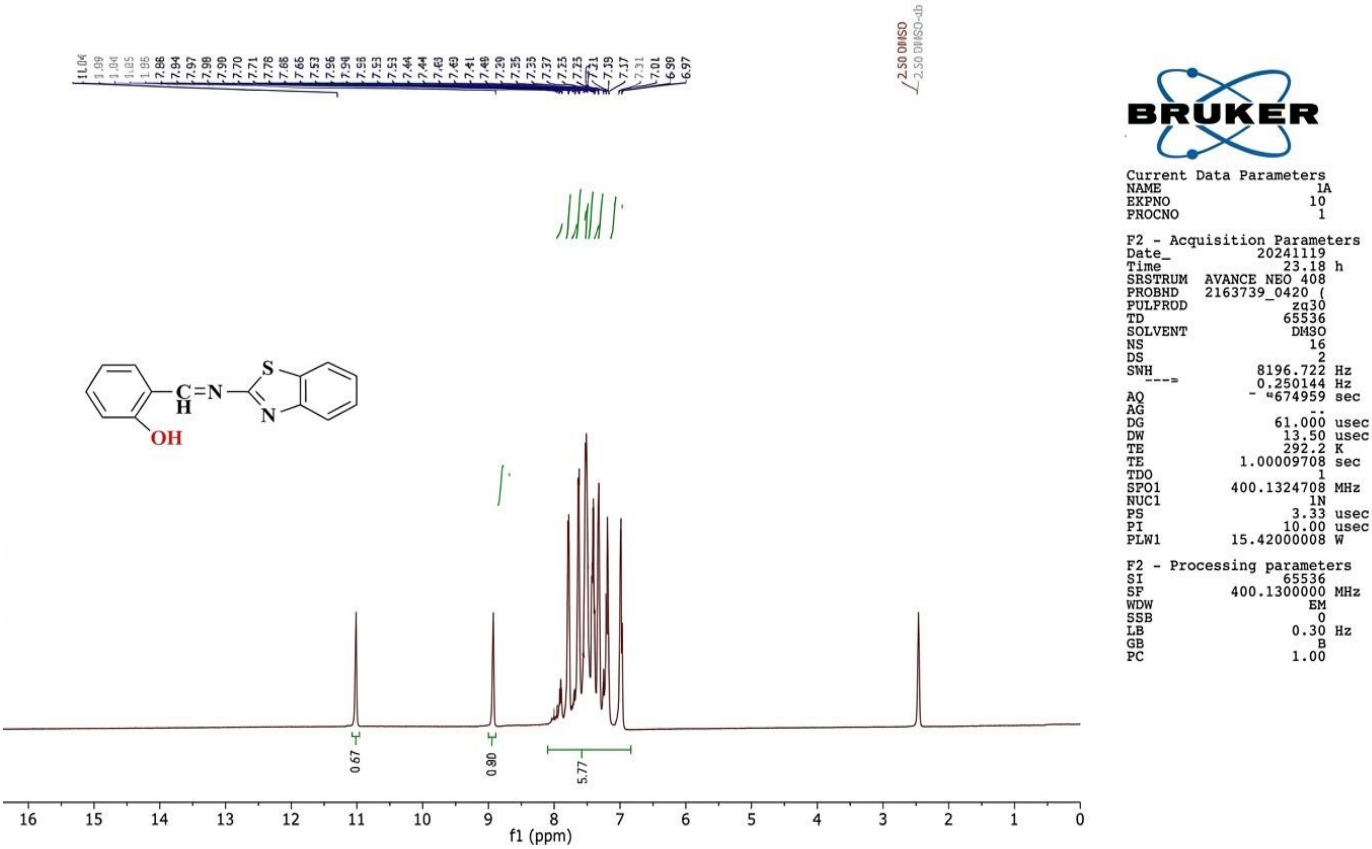


Figure 11. ^{1}H-NMR spectrum of the ligand L1.
Source: Elaborated by the authors.

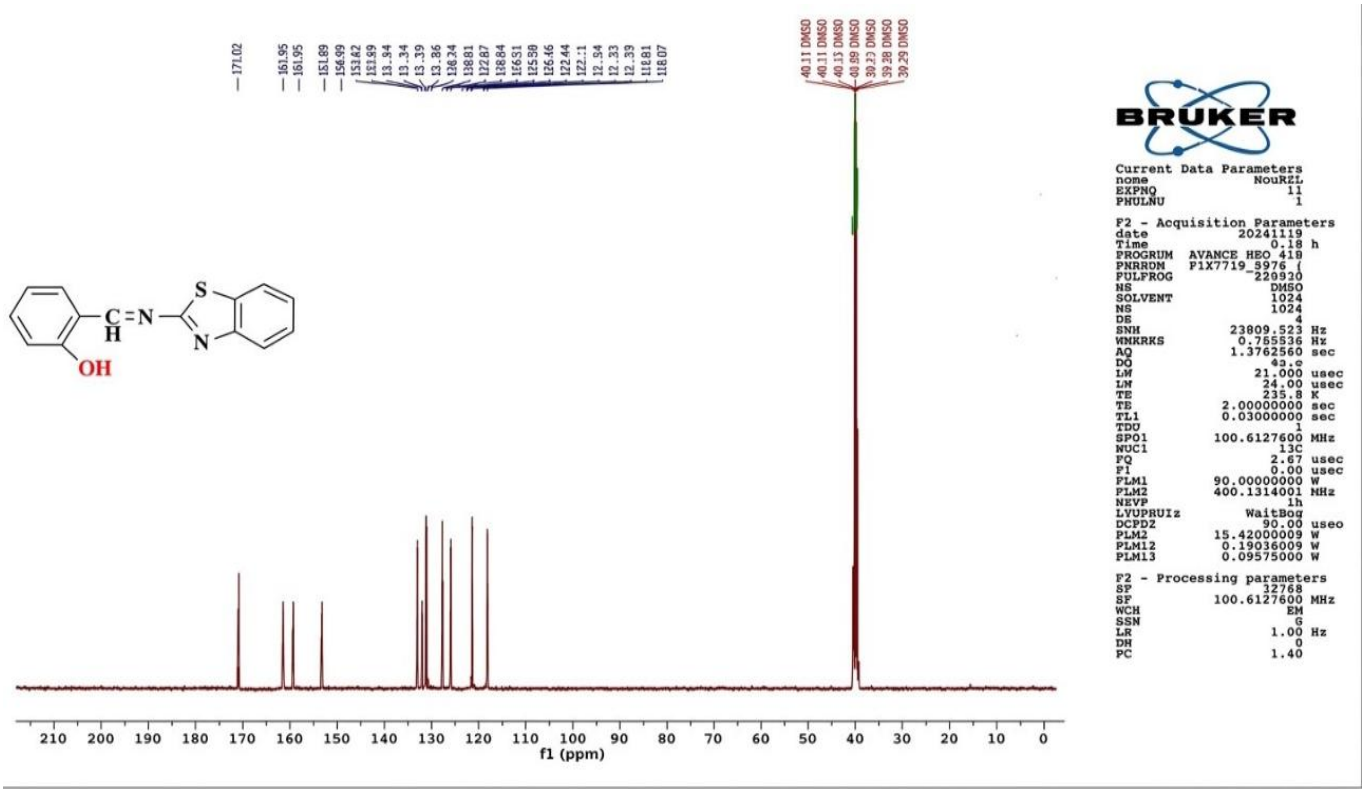


Figure 12. C^{13}-NMR spectrum of the ligand L1.
Source: Elaborated by the authors.

3.8. Thermogravimetric analysis

The thermal behavior of the selectively prepared complex was studied at a heating rate of 25 °C per minute in a temperature range of 30–500 °C to confirm if the complex was free of water. The thermogram (**Fig. 13**) exhibits two distinct weight-loss stages, indicating a two-step thermal decomposition process. The first stage is associated with the initial decomposition process, while the second and subsequent weight loss can be attributed mainly to the progressive decomposition of the organic ligand (L1) and the possible elimination of chloride ions. No distinct weight-loss step attributable to the loss of lattice or coordinated water molecules was observed at low temperatures, supporting the anhydrous nature of the complex. At higher temperatures, the remaining residue is tentatively assigned to zinc oxide (ZnO), based on the expected thermal decomposition pathway of Zn(II) complexes. In contrast, the thermograms presented in (**Figs. 14–17**) exhibit a single major weight-loss stage for each corresponding complex. These weight-loss stages are attributed mainly to the thermal decomposition of the organic components of the complexes, together with the possible elimination of chloride or other coordinated/ionic species, depending on the composition of each complex. No distinct low-temperature weight loss attributable to lattice or coordinated water molecules was observed in these complexes, supporting their anhydrous nature. At higher temperatures, the remaining residues are attributed to the corresponding metal-containing inorganic products formed after thermal decomposition. Overall, the TGA results provide evidence for the thermal decomposition behavior of the investigated complexes and support the proposed anhydrous nature of the complexes (Mohamed *et al.*, 2024).

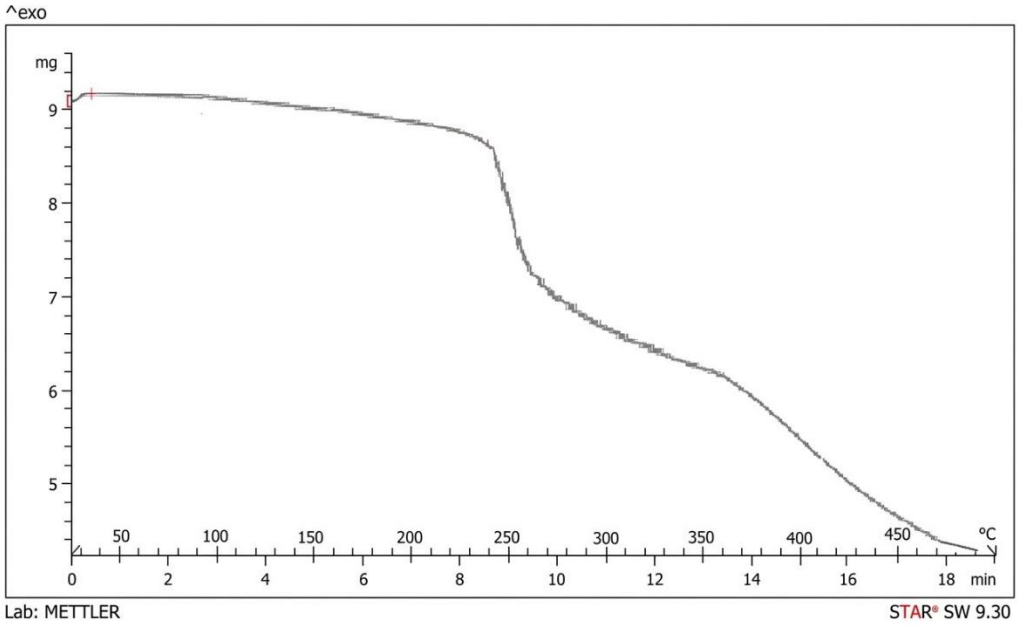


Figure 13. Thermogravimetric analysis (TGA) of the complex $[Co(L1)_2]Cl_2$.
Source: Elaborated by the authors.

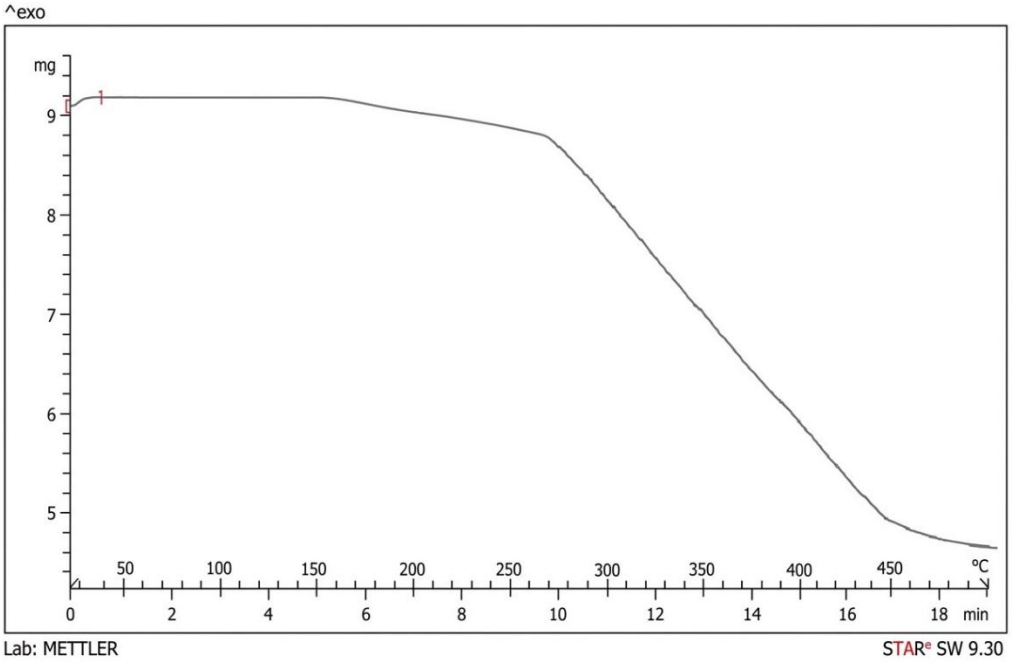


Figure 14. Thermogravimetric analysis (TGA) of the complex $[Ni(L1)_2]Cl_2$.
Source: Elaborated by the authors.

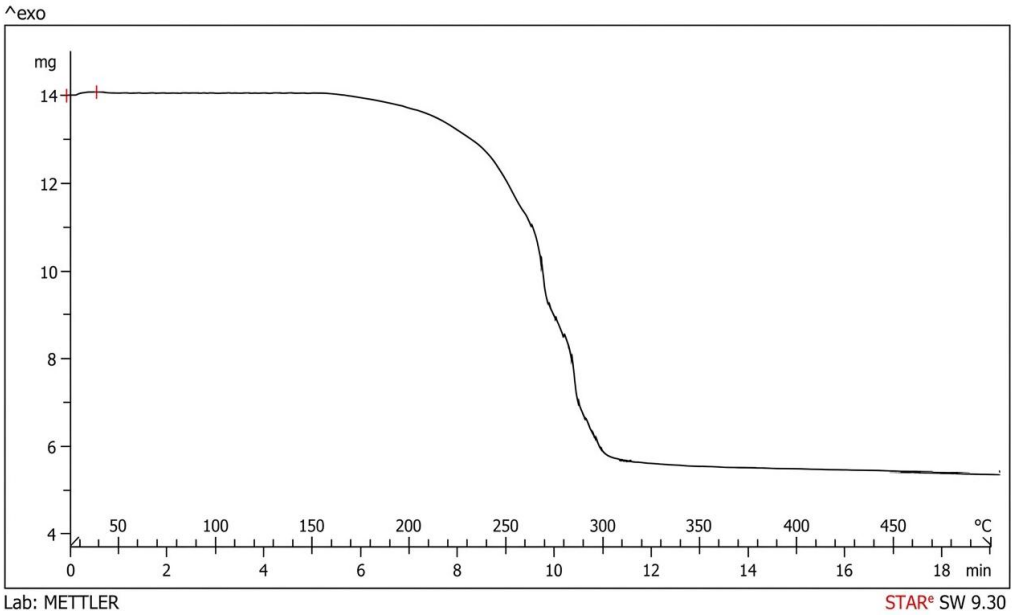


Figure 15. Thermogravimetric analysis (TGA) of the complex $[Cu(L1)_2]Cl_2$.
Source: Elaborated by the authors.

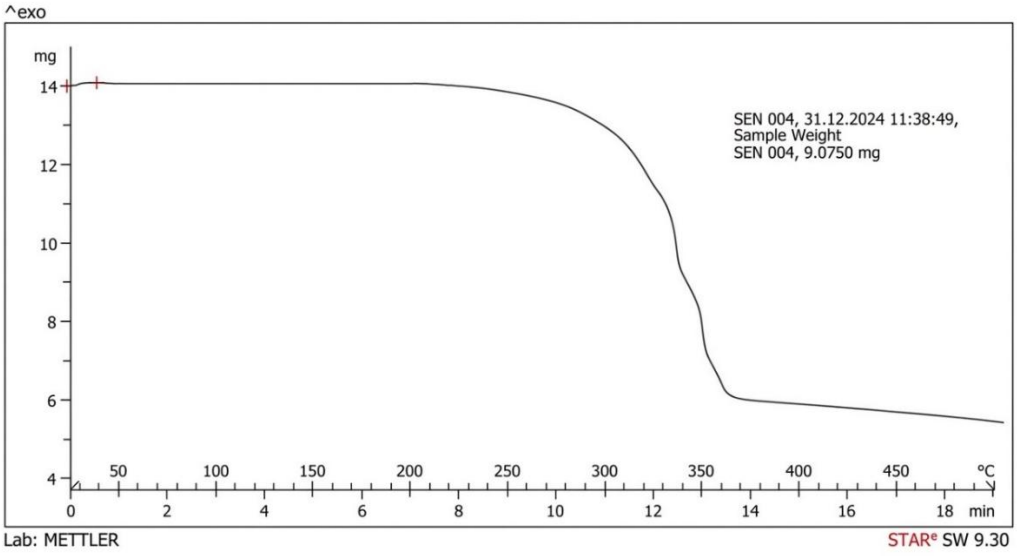


Figure 16. Thermogravimetric analysis (TGA) of the complex $[Zn(L1)_2]Cl_2$.
Source: Elaborated by the authors.

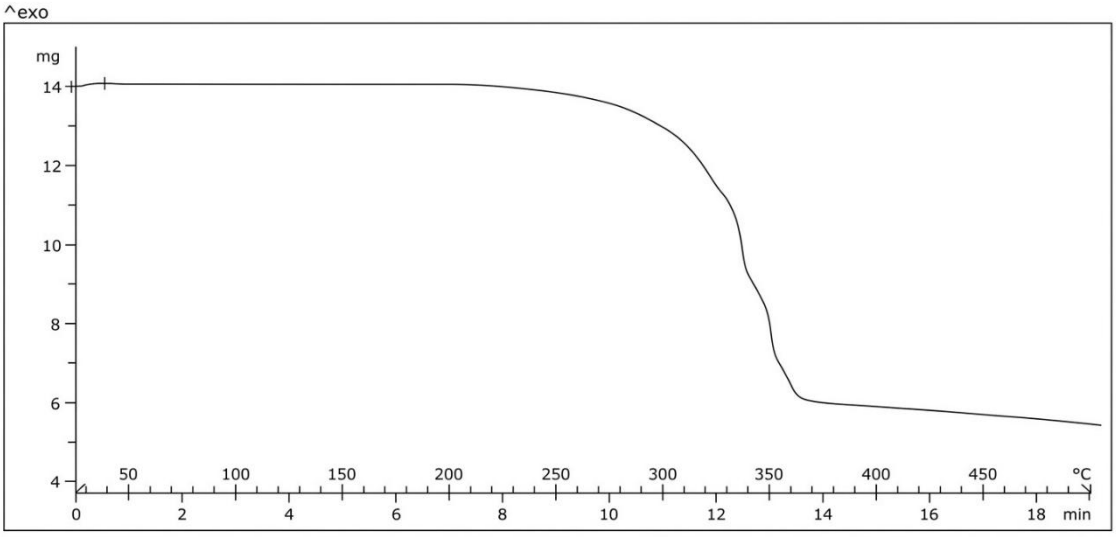


Figure 17. Thermogravimetric analysis (TGA) of the complex $[Zn(L1)_2]Cl_2$.
Source: Elaborated by the authors.

https://doi.org/10.26850/1678-4618.eq.v51.2026.e1660

3.9. Mass spectrum

The characterization performed in this study was primarily intended to confirm the formation of the metal–ligand complexes, verify the increase in molecular mass upon coordination, and confirm the proposed molecular formulae. The mass spectra of ligand (L1) and zinc complex (complex 4) were measured, and data are in **Table 4**. The mass spectrum of the ligand (L1) shows a prominent molecular ion peak at 254 m/z, corresponding to the molecular weight of the ligand (**Fig. 18**). This confirms the successful synthesis and purity of the ligand. For the zinc complex $[Zn(L1)_2]Cl_2$ (**Fig. 19**), the molecular ion peak appears at 644 m/z, which matches the expected molecular weight of the complex minus the chloride ions (due to fragmentation in the mass spectrometer). Fragmentation pathways likely involve the sequential cleavage of the ligand moieties or loss of small neutral molecules (e.g., H_2O, Cl), leading to characteristic fragment ions. These fragmentation patterns support the proposed structure of both the ligand and its zinc complex (Abd El-Lateef *et al.*, 2024).

Table 4. Mass spectra data of the ligand and the metal(II) complexes.

NO	Fragment	Mass/charge (m/z)
	L1	
1	$[C_{14}H_{10}N_2SO]^+$	253
2	$[C_7H_5SN]^+$	139
3	$[C_7H_5N]^+$	131
4	$[C_6H_5N]^+$	111
5	$[C_5H_6N]^+$	96
	$[Zn(L1)_2]Cl_2$	
1	$[C_{28}H_{19}N_4S_2O_2Zn]^+$	611
2	$[C_{28}H_{17}N_4SO_2]^+$	435
3	$[C_{14}H_{10}N_2SO]^+$	253
4	$[C_7H_5ClN]^+$	139
5	$[C_7H_4NS]^+$	130
6	$[C_6H_4O]^+$	111
7	$[C_7H_4N]^+$	96
8	Zn^+	65

Source: Elaborated by the authors.

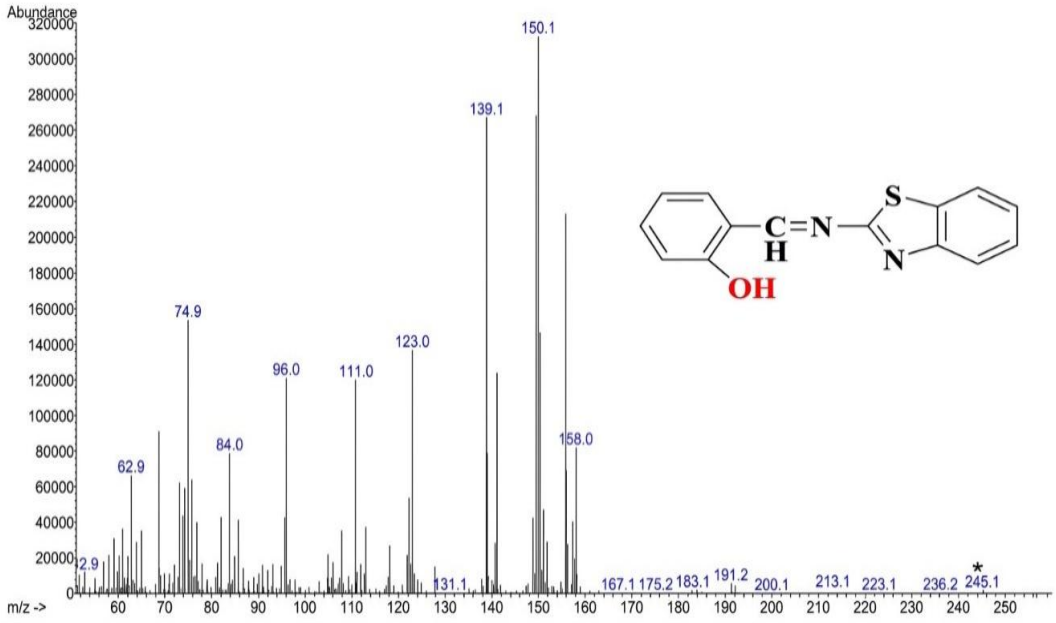


Figure 18. Mass spectrum of the ligand.
Source: Elaborated by the authors.

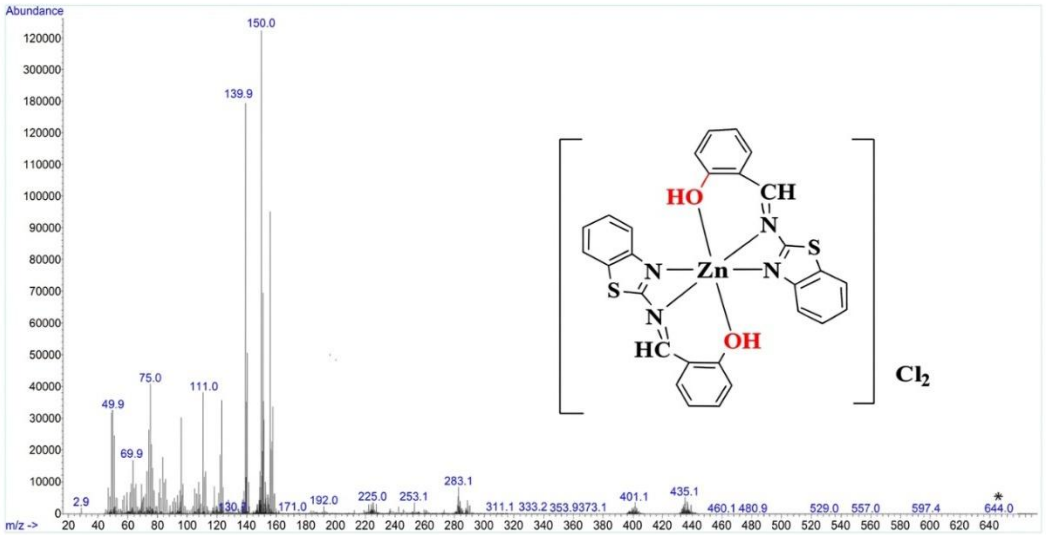


Figure 19. Mass spectrum of complex 4.
Source: Elaborated by the authors.

3.10. Biological activity

The effect of the prepared ligand and complexes on two types of bacteria, *Staphylococcus aureus* (gram-positive) and *Pseudomonas aeruginosa* (gram-negative), was studied using the well-drilling method.

These bacteria were chosen due to their importance in medicine, as they cause many diseases. In addition, they exhibit a distinct form of resistance to antibiotics and therapeutic chemicals (Chavan and Patil, 2024). The results in **Table 5** and **Fig. 20** indicate that most of the compounds prepared in the laboratory inhibit the bacteria used. It has been proven to have an inhibitory effect against these types of bacteria.

Table 5. Antibacterial activity (inhibition zone) of the ligand and complexes.

Compound	*Staphylococcus aureus*	*Pseudomonas aeruginosa*
L1	16	20
1	20	20
2	19	21
3	19	19
4	21	22
CIPS	10	10
TMP	12	10

Source: Elaborated by the authors.

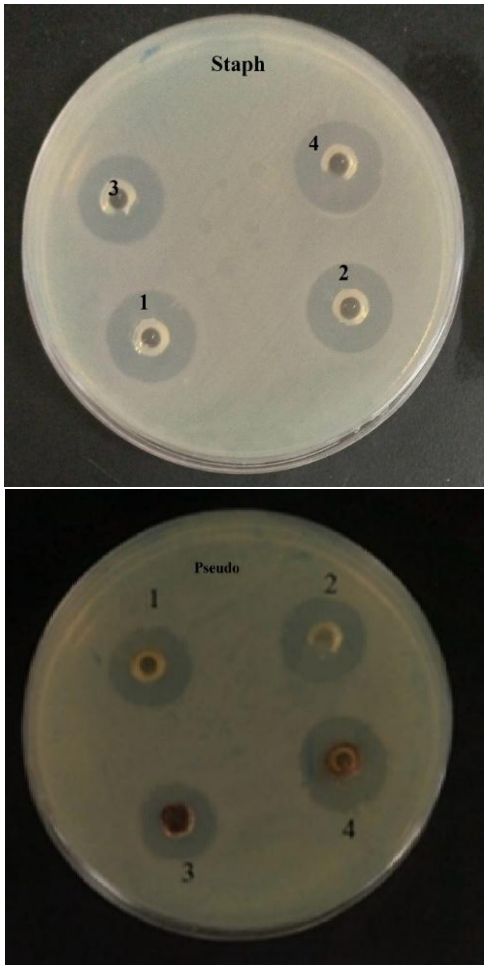


Figure 20. The biological activity of ligands and complexes against *Staphylococcus aureus, Pseudomonas aeruginosa* bacteria at a concentration of (10^{-3} mol L^{-1}).
Source: Elaborated by the authors.

The biological activity of the Schiff base complexes Co(II), Ni(II), Cu(II), Zn(II) stems from three synergistic mechanisms:

1-Membrane Disruption: The benzothiazole moiety with S-N donors and aromatic rings enhances lipophilicity, facilitating penetration into bacterial membranes, especially Gram-negative. Metal ions Zn(II) disrupt ion gradients by forming non-specific channels.

2-Enzyme Inhibition: Metal coordination Cu(II) competitively inhibits metalloenzymes (DNA gyrase) by displacing essential ions (Mg^{+2}-Ca^{+2} or binding to thiol (-SH groups).

3-Oxidative Stress: Redox-active metals Cu(II)-Co(II) generate ROS, OH, and O_2^-, damaging DNA and lipids. Zn(II) complexes indirectly induce oxidative stress by depleting cellular antioxidants (Abd El-Lateef et al., 2024; Abed et al., 2021; Aziz et al., 2023; Chavan and Patil, 2024; Gavali et al., 2024; Mansour et al., 2024).

4. Conclusions

According to the analytical, physical, and spectroscopic results, the observed data revealed the following:

A) Complexes with a molar ratio of (1:2) were octahedral, symmetrical, and had the formula $[M(L1)_2]Cl_2$.

B) The biological activity of the ligand and its complexes show that they have excellent antimicrobial properties.

Authors' contribution

Conceptualization:Fadia Jalal Ahmed; **Data curation**: Sondos Ibrahim Atallah; **Formal Analysis**: Sondos Ibrahim Atallah; **Funding acquisition**: Not applicable; **Investigation**: Sondos Ibrahim Atallah; **Methodology**: Fadia Jalal Ahmed; **Project administration**: Fadia Jalal Ahmed; **Resources**: Fadia Jalal Ahmed; **Software**: Not applicable; **Supervision**: Fadia Jalal Ahmed; **Validation**: Fadia Jalal Ahmed; **Visualization**: Sondos Ibrahim Atallah; **Writing – original draft**: Sondos Ibrahim Atallah; **Writing – review & editing**: Fadia Jalal Ahmed.

Conflict of interest

The authors declare that there is no conflict of interest.

Data availability statement

All data sets were generated or analyzed in the current study.

Artificial Intelligence usage statement

The authors declare that they did not use Artificial Intelligence tools at any stage of the preparation, correction, or evaluation of this work, including Graphical Abstract preparation.

Funding

Not applicable.

Acknowledgments

The authors would like to express their sincere gratitude to the Department of Chemistry, College of Education for Pure Sciences, University of Mosul, for providing the necessary facilities to conduct this research. Special thanks are also extended to the University of Basrah and the University of Tehran laboratories for their assistance in conducting spectroscopic and elemental analyses.

References

Abd El-Lateef, H. M.; Ali, A. M.; Khalaf, M. M.; Abdou, A. New iron (III), cobalt (II), nickel (II), copper (II), zinc (II) mixed-ligand complexes: Synthesis, structural, DFT, molecular docking and antimicrobial analysis. *Bulletin of the Chemical Society of Ethiopia.* **2024**, *38* (1), 147–166. https://doi.org/10.4314/bcse.v38i1.12

Abed, R. R.; Ahmed, F. J.; Raoof, S. A. New Cu (II) and Zn (II) complexes with O-nitrobenzylidene trimethoprim, Evaluation of their Antibacterial activities. Proceedings of the 1st International Multi-Disciplinary Conference Theme: Sustainable Development and Smart Planning, IMDC-SDSP 2020, Cyperspace, 28-30 June 2020. https://doi.org/10.4108/eai.28-6-2020.2298121

Abed, R. R.; Mohammed, A. S.; Ahmed, F. J. Synthesis and diagnoses of new metal ions complexes derived from trimethoprim schiff bases. *Research Journal of Pharmacy and Technology.* **2021**, *14* (9), 4963–4968. https://doi.org/10.52711/0974-360X.2021.00863

Abousaty, A. I.; Reda, F. M.; Hassanin, W. A.; Felifel, W. M.; El-Shwiniy, W. H.; Selim, H. M.; Bendary, M. M. Sorbate metal complexes as newer antibacterial, antibiofilm, and anticancer compounds. *BMC microbiology.* **2024**, *24* (1), 262. https://doi.org/10.1186/s12866-024-03370-w

Adnan, T. K.; Ahmed, K. Y.; Jarullah, A. A. Synthesis and application of new Co/Cu/Ni/Zn (II) Schiff base complexes in the biological activity and oxidation of alcohols. *Iranian Journal of Catalysis.* **2024**, *14* (3), 142426. https://doi.org/10.57647/j.ijc.2024.1403.26

Afifi, M. A.; Rasmy, A. A.; Elzayat, E. M.; El-Medani, S. M.; Shehata, M. R.; Elantabli, F. M. Spectroscopic, docking, antiproliferative, and anticancer activity of novel metal derivatives of phenylacetohydrazide Schiff base on different human cancer cell lines. *BMC Chem.* **2025**, *19* (1), 69. https://doi.org/10.1186/s13065-025-01417-1

Ahmed, F. J.; AbdAlqader, B.; Haddad, R. A.; Abed, R. R.; Saleh, M. Y. Preparation and diagnosis of Zn (II), Cd (II) and Hg (II) complexes with Schiff base ligand derived from trimethoprim. *Egyptian Journal of Chemistry.* **2022**, *65* (10), 359–366. https://doi.org/10.21608/EJCHEM.2022.119210.5362

Alkam, H. H. Synthesis and Characterization of New Bidentate Schiff Base Ligand Type (NO) Donor Atoms Derived from Isatin and 3-Amino Benzoic Acid and Its Complexes with Co (II), Cu (II), Cd (II) and Hg (II) Ions. *Ibn AL-Haitham Journal For Pure and Applied Science.* **2017**, *30* (3), 158–169. https://doi.org/10.30526/30.3.1610

Almáši, M.; Vilková, M.; Bednarčík, J. Synthesis, characterization and spectral properties of novel azo-azomethine-tetracarboxylic Schiff base ligand and its Co (II), Ni (II), Cu (II) and Pd (II) complexes. *Inorganica Chimica Acta.* **2021**, *515*, 120064. https://doi.org/10.1016/j.ica.2020.120064

Aziz, T.; Nasim, H. A.; Ahmad, K.; Shah, H.-u.-R.; Parveen, S.; Ahmad, M. M.; Majeed, H.; Galal, A. M.; Rauf, A.; Ashfaq, M. Rational synthesis, biological screening of azo derivatives of chloro-phenylcarbonyl diazenyl hydroxy dipyrimidines/thioxotetrahydropyrimidines and their metal complexes. *Heliyon.* **2023**, *9* (1), e12492. https://doi.org/10.1016/j.heliyon.2022.e12492

Butera, V.; D'Anna, L.; Rubino, S.; Bonsignore, R.; Spinello, A.; Terenzi, A.; Barone, G. How the Metal Ion Affects the 1H NMR Chemical Shift Values of Schiff Base Metal Complexes: Rationalization by DFT Calculations. *The Journal of Physical Chemistry A.* **2023**, *127* (44), 9283–9290. https://doi.org/10.1021/acs.jpca.3c05653

Chavan, J. K.; Patil, R. M. Synthesis, Spectroscopic and Biological Activity Studies of Zinc(II) Complexes of N1, N'4-bis ((1E, 2E)-2-(hydroxyimino)-1-(4-R)-phenylethylidene) terephthalohydrazide Schiff base. *Oriental Journal of Chemistry.* **2024**, *40* (3), 689–697. https://doi.org/10.13005/ojc/400308

Dalia, S. A.; Afsan, F.; Hossain, M. S.; Khan, M. N.; Zakaria, C.; Zahan, M.-E.; Ali, M. A short review on chemistry of schiff base metal complexes and their catalytic application. *Int. J. Chem. Stud.* **2018**, *6* (3), 2859–2867.

Gavali, L. V.; Mohammed, A. A.; Al-Ogaili, M. J.; Gaikwad, S. H.; Kulkarni, M.; Das, R.; Ubale, P. A. Novel terephthalaldehyde bis (thiosemicarbazone) Schiff base ligand and its transition metal complexes as antibacterial Agents: Synthesis, characterization and biological investigations. *Results in Chemistry.* **2024**, *7*, 101316. https://doi.org/10.1016/j.rechem.2024.101316

Hamil, A.; El-ajaily, M.; Basher, L.; Miloud, M.; Saad, S. Mixed ligand chelates using Schiff base and 2-aminobenzoic acid as ligands. *Libyan Journal of Medical Research.* **2024**, *18* (1), 1–17. https://doi.org/10.54361/10.26719/llmr18-1.01

Ismail, A. A.; Lateef, S. M. Structural, characterization, and biological activity of novel schiff base ligand derived from pyridoxal with 2-aminobenzothazol and its complexes. *Chemical Methodologies*. **2022**, *6*, 1007–1022. https://doi.org/10.22034/chemm.2022.357804.1600

Khalil, E.; Mahmoud, W.; Mohamed, G. Synthesis, spectral, thermal and biological studies of some transition and inner transition Schiff base metal complexes. *Egyptian Journal of Chemistry.* **2021**, *64* (7), 3555–3571.

Khalil, M. H.; Abdullah, F. O. Synthesis, characterisation, and anticancer and antioxidant activities of novel complexes of palladium and an organic Schiff-base ligand. *Bulletin of the Chemical Society of Ethiopia.* **2024**, *38* (3), 605–613. https://doi.org/10.4314/bcse.v38i3.5

Knittl, E. T.; Abou-Hussein, A. A.; Linert, W. Syntheses, characterization, and biological activity of novel mono- and binuclear transition metal complexes with a hydrazone Schiff base derived from a coumarin derivative and oxalyldihydrazine. *Monatsh Chem.* **2018**, *149* (2), 431–443. https://doi.org/10.1007/s00706-017-2075-9

Mansour, M.; Abd-Elkarim, A. T.; Mahmoud, W. H.; El-Sherif, A. A. Quinazoline-Glycine Manganese (II) Nano-Complex for Arsenic Sensing via QCM: Synthesis, Characterization, DFT Studies, Biological Evaluation and Environmental Application. *Egyptian Journal of Chemistry*. **2024**. https://doi.org/10.21608/ejchem.2024.294794.9796

Mohamed, E. A.; Ali, A. E.; Kolkaila, S. A.; Fyala, S. S.; Elasala, G. S. Synthesis, Spectroscopic Studies, Thermal Analysis and Molecular Docking of Chloramphenicol Metal Complexes as Anti-Prostate Cancer. *TWIST.* **2024**, *19* (1), 400–408.

Mukhtar, S. S.; Hassan, A. S.; Morsy, N. M.; Hafez, T. S.; Hassaneen, H. M.; Saleh, F. M. Overview on synthesis, reactions, applications, and biological activities of Schiff bases. *Egyptian Journal of Chemistry.* **2021**, *64* (11), 6541–6554.

Oladipo, S. D.; Luckay, R. C. Copper (II) complexes derived from naphthalene-based halogenated Schiff bases: Synthesis, structural analysis, DFT computational studies and in vitro biological activities. *New Journal of Chemistry.* **2024**, *48* (30), 13276–13288. https://doi.org/10.1039/D4NJ01621A

Ommenya, F.; Nyawade, E.; Andala, D.; Kinyua, J. Synthesis, Characterization and Antibacterial Activity of Schiff Base, 4-Chloro-2-{(E)-[(4-Fluorophenyl) imino] methyl} phenol Metal (II) Complexes. *Journal of Chemistry.* **2020**, *2020* (1), 1745236. https://doi.org/10.1155/2020/1745236

Paul, T.; Hossen, M. F. Schiff base metal complexes: Synthesis, characterization, thermal analysis and antibacterial activity. *Asian Journal of Research in Chemistry.* **2020**, *13* (4), 265–274. https://doi.org/10.5958/0974-4150.2020.00052.8

Radhi, E. R.; Ali, F. J.; Ali, K. J. Synthesis and characterization of a new azo quinoline ligand and its metal complexes with spectrophotometric determination and biological efficacy study of its Hg (II) complex. *Bulletin of the Chemical Society of Ethiopia.* **2023**, *37* (6), 1423–1433. ttps://doi.org/10.4314/bcse.v37i6.10

Raj, J.; Jain, A.; Sharma, N.; Kumari, A.; Fahmi, N. Synthesis, spectral characterization, and biological activities of novel palladium (II) and

platinum (II) complexes of active Schiff base ligands. *Bulletin of the Chemical Society of Ethiopia.* **2023**, *37* (6), 1383–1396. https://doi.org/10.4314/bcse.v37i6.7

Rana, A. K.; Parekh, N. R.; Dabhi, H. R.; Nadkarni, S. S. Novel Synthesis and Characterization of Thiosemicarbazone Compounds Containing 4-Acyl-2-pyrazolin-5-ones. *Journal of Chemistry,* **2009**, *6* (3), 747–752. https://doi.org/10.1155/2009/472530

Soliman, A. I. A.; Sayed, M.; Elshanawany, M. M.; Younis, O.; Ahmed, M.; Kamal El-Dean, A. M.; Abdel-Wahab, A. A.; Wachtveitl, J.; Braun, M.; Fatehi, P.; Tolba, M. S. Base-Free Synthesis and Photophysical Properties of New Schiff Bases Containing Indole Moiety. *ACS omega.* **2022**, *7* (12), 10178–10186. https://doi.org/10.1021/acsomega.1c06636

Srivastava, K.; Singh, A.; Singh, S. K. Green and efficient synthesis, characterization and antibacterial activity of Copper (II) complexes with unsymmetrical bidentate Schiff base ligands. *IOSRJ. Appl. Chem.* **2014**, *7* (4), 16–23. https://doi.org/10.9790/5736-07411623

Sultan, M.; Hassan, S. S.; Omran, K.; Hassan, H. A novel Ni–Schiff base complex for motivating glucose electrooxidation in alkaline solutions. *Materials Advances.* **2024**, *5* (3), 1264–1283. https://doi.org/10.1039/D3MA00730H

Tahmasbi, A.; Jafari, A.; Nikoo, A. Synthesis, characterization, and nonlinear optical properties of copper (II) ligand Schiff base complexes derived from 3-Nitrobenzohydrazide and benzyl. *Sci Rep.* **2023**, *13* (1), 10988. https://doi.org/10.1038/s41598-023-38086-w

Uttu, A. J.; Sallau, M. S.; Iyun, O. R. A.; Ibrahim, H. Isolation, characterization and in silico molecular docking studies of two terpenoids from Strychnos innocua Delile root bark for antibacterial properties. *Adv. J. Chem. Sect. A.* **2022**, *5*, 241–252.

Zahradnikova, E.; Pichon, C.; Duhayon, C.; Sutter, J. P.; Halas, P.; Drahos, B. Synthesis, structural and magnetic properties of cobalt(ii) complexes with pyridine-based macrocyclic ligand containing two pyridine pendant arms. *RSC Adv.* **2024**, *14* (38), 28138–28147. https://doi.org/10.1039/d4ra02387k